



Electroseparation of zinc(II) from uranium(III) prepared by reduction of uranium(IV) with zinc amalgam in dimethylformamide

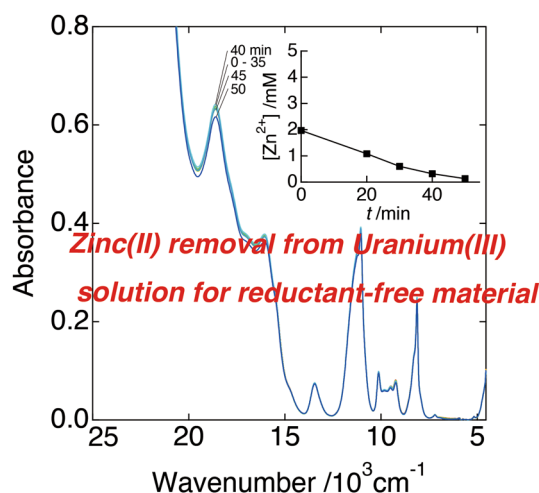
Kenji Shirasaki¹

Received: 1 August 2021 / Accepted: 26 March 2022 / Published online: 10 April 2022
© The Author(s), under exclusive licence to Springer Nature B.V. 2022

Abstract

The Electroseparation of zinc(II) from a solution of uranium(III) generated by the reduction of uranium(IV) triflate ($\text{U}(\text{OTf})_4$) with zinc amalgam ($\text{Zn}(\text{Hg})$) was studied to establish a convenient route to the precursors of organic uranium(III) compounds. Specifically, the electrode reactions of $\text{U}(\text{OTf})_4$ in N,N -dimethylformamide on mercury (Hg) and $\text{Zn}(\text{Hg})$ electrodes were probed by voltammetry and bulk electrolysis measurements. The voltammograms recorded on the former electrode showed three cathodic waves assigned to the reduction of a uranium(IV) solvate complex (-1.48 V), the reduction of $[\text{U}(\text{OTf})]^{3+}$ (-1.81 V), and uranium amalgamation (-2.65 V). On the latter electrode, the first cathodic wave was masked, as it was located at the potential of zinc amalgamation. Bulk electrolysis experiments revealed that for both Hg and $\text{Zn}(\text{Hg})$, the working electrode potential featured a plateau around -2.3 V, which was not observed in the corresponding voltammograms and was related to the degradation of uranium(III) based on spectroscopic observations. The Electroseparation of zinc(II) from the uranium(III) solution on $\text{Zn}(\text{Hg})$ was successfully (highest coulombic efficiency = 0.81, final zinc(II) separation ratio = 93.4%) carried out after the reduction of $\text{U}(\text{OTf})_4$ by $\text{Zn}(\text{Hg})$.

Graphical abstract



Keywords Uranium(III) · Electroseparation · Zinc amalgamation · Voltammetry · Bulk electrolysis

✉ Kenji Shirasaki
kenji.shirasaki.e4@tohoku.ac.jp

¹ Institute for Materials Research, Tohoku University, Sendai, Miyagi 980-8577, Japan

1 Introduction

The past two decades have witnessed a revival of interest in low-valent uranium chemistry, such as the unusual reactions mediated by uranium(III) [1–8]. As further development

in this field relies on the availability of uranium(III) compounds, the establishment of their convenient syntheses has drawn much attention [9–12].

Uranium(III) species (e.g., U^{III} and $\text{U}(\text{OTf})_3$) and their solvent adducts are typically prepared from uranium metal [9, 11, 13–15], while other routes such as the reduction of uranium(IV) by metals [16, 17] or other agents [18–26] are less common. These alternative routes are appropriate for the synthesis of compounds such as $\text{UL}_4(\text{Ph}_4\text{B})_3$ (L = amide derivative) [18], $\text{LiU}_2\text{Cl}_7(\text{THF})_{4,5}$ (THF = tetrahydrofuran) [21], and $\text{U}(\text{L}')_3$ (L' = *N,N*-dimethylaminodiboranate) [25] but are not practical in other cases because of the difficulty of separating the spent reducing agent from uranium(III) products. The most convenient and common reductant for this purpose is zinc amalgam ($\text{Zn}(\text{Hg})$) [26], which has been used for the preparation of uranium(III) species from uranium(IV) and uranyl(VI) in aqueous [27, 28] and organic solutions [29, 30] and for the study of their electrochemical and spectroscopic properties. Previously, we evaluated the stability of uranium(III) prepared by the reduction of $\text{U}(\text{OTf})_4$ with $\text{Zn}(\text{Hg})$ in THF and found that the uranium(III) oxidation state could be maintained for more than a week when the solution was kept in contact with $\text{Zn}(\text{Hg})$, whereas gradual oxidation was observed in the absence of $\text{Zn}(\text{Hg})$ [31]. Therefore, uranium(III) compounds with various counter ions can be conveniently prepared if zinc(II) eluted from $\text{Zn}(\text{Hg})$ can be rapidly removed from uranium(III) solutions in organic solvents.

Selective reduction relies on the differences in solute redox potentials and has been used in numerous bulk electrolysis-based electroseparations, as exemplified by the removal of > 96 wt% of aluminum impurities from LiCl-KCl melts [32] and that of ~95% of CaCl_2 from $\text{CaCl}_2\text{-LiCl-KCl}$ melts [33] prior to lithium(I) reduction as well as by the separation of uranium from lanthanides in LiCl-KCl melts on a liquid gallium electrode [34]. The above technique was also used for the removal of non-metallic impurities such as oxygen, sulfur, and selenium from molten copper [35] and the removal of bromate using boron-doped diamond electrodes [36]. Although the bulk electrolysis of uranium solutions has been widely studied for various purposes, e.g., direct recovery for spent nuclear fuel reprocessing [34, 37–42], the solution-phase Electroseparation of zinc(II) from uranium(III) remains underexplored.

The electrochemistry of zinc and low-valent uranium has been studied using the mercury (Hg) electrode in aqueous and organic solutions. The behavior of zinc(II) on this electrode can be simply explained by amalgamation and dissolution irrespective of the solution composition [43–45], while the electrode reactions of low-valent uranium are strongly influenced by both the solvent and the electrolyte. In polarographic studies of UCl_4 , two cathodic waves assigned to the reversible reduction of uranium(IV) to uranium(III) and

irreversible uranium amalgamation were observed at -1.13 and -1.93 V vs. the standard calomel electrode (-1.52 and -2.32 V vs. Ag/Ag^+) in dimethylformamide (DMF), respectively; whereas both of these reactions were irreversible in dimethyl sulfoxide (DMSO) [46]. Two irreversible cathodic waves were also observed on a hanging mercury electrode (HME) when a solution of $\text{U}(\text{ClO}_4)_4$ in DMSO was probed by cyclic voltammetry (CV) [47]. In the bulk electrolysis of uranium(IV) in DMF, the electrode reactions are also strongly dependent on the electrode material and counter ion, e.g., in the case of the Hg pool electrode and perchlorate as the counter ion, the electrode potential stays at -1.4 V vs. Fc/Fc^+ (-1.4 V vs. Ag/Ag^+), whereas a plateau at -2.2 V vs. Fc/Fc^+ (-2.2 V vs. Ag/Ag^+) is observed for triflate as the counter ion. In both cases, the intensity of the uranium(IV) absorption band decreases with time at the plateau, whereas that of the uranium(III) band initially increases and then saturates or decreases at the same plateau [48].

To shed light on the electrochemical behavior of low-valent uranium triflate, we probed the electrode reactions of $\text{U}(\text{OTf})_4$ by voltammetry, using the standard HME and that where Hg was substituted by $\text{Zn}(\text{Hg})$. This study used DMF with its large negative potential window [49] as a solvent and tetrabutylammonium triflate (TBAOTf) as a supporting electrolyte. For comparison, we also probed the bulk electrolysis of $\text{U}(\text{OTf})_4$ in the presence of zinc(II) in DMF containing TBAOTf on both the pool Hg and the $\text{Zn}(\text{Hg})$ electrodes. The Electroseparation of zinc(II) from the uranium(III) solution prepared by the reduction of $\text{U}(\text{OTf})_4$ on $\text{Zn}(\text{Hg})$ in DMF was studied for the first time to evaluate the possibility of the convenient preparation of spent reductant-free uranium(III) starting materials.

2 Experimental

2.1 Materials

DMF was purchased from Fujifilm Wako Pure Chemical Corporation and distilled under reduced pressure before use. TBAOTf was purchased from Tokyo Kasei Kogyo Co., Ltd. (Tokyo, Japan) and used without further purification. Other chemicals, except for UO_3 , were used as received (Fujifilm Wako Pure Chemical Corporation). Deionized water (18 M Ω cm, Academic A10 model, Milli-Q, USA) was used in all experiments. $\text{Zn}(\text{Hg})$ was prepared as described elsewhere [28]. Briefly, zinc tips (3 g) were reacted with Hg (100 g) in 0.5 M aqueous H_2SO_4 for 1 h at 343 K, and the resulting product was washed with dry DMF (5 \times 20 mL) to remove residual water.

$\text{U}(\text{OTf})_4$ was prepared as follows. UO_3 (5.72 g) was dissolved in aqueous triflic acid (12.3 mL $\text{CF}_3\text{SO}_3\text{H}$ + 10 mL H_2O) at 353 K and the solution was electroreduced on a Hg

cathode at a constant voltage to afford uranium(IV). The product obtained after the evaporation of the obtained solution was dried in vacuo for 12 h at 453 K and for a further 3 h in a flow of dry N_2 gas. The resulting green dendritic crystals were examined by elemental analysis (Flash EA1112 CHN analyzer, Thermo Quest Italia) and inductively coupled plasma-atomic emission spectrometry (ICP-AES; ICP-7500, Shimadzu Corp., Japan), and their composition was determined as $U(OTf)_4$ (calcd.: U, 28.53 wt%; C, 5.76 wt%; H, 0.00 wt%; found: U, 28.36 wt%; C, 6.14 wt%; H, 0.00 wt%).

The uranium(III) solution used for electrochemical zinc(II) removal was prepared by the reduction of $U(OTf)_4$ over Zn(Hg) in DMF and the obtained solution was promptly used to determine the molar extinction coefficients of the uranium(III) absorption bands (Fig. S1).

2.2 Methods

All experiments were carried out inside an Ar-filled glove box (< 1 ppm O_2 and H_2O) at room temperature. CV and normal pulse voltammetry (NPV) measurements were performed using a three-electrode system (HZ-3000 and HZ-7000, Hokuto Denkou Corp., Japan). The working electrode (WE) was either the HME (Yanako Co. Ltd., Japan) or a Zn(Hg) electrode obtained by substituting Hg in the HME for Zn(Hg) (electrolyte contact area $\approx 1.4 \text{ mm}^2$). The counter electrode (CE) was a 10 mm \times 10 mm Pt plate. The Ag/Ag^+ reference electrode (RE) comprised a silver wire and a solution of $AgNO_3$ (0.01 M) and TBAOTf (0.1 M) in freshly prepared DMF. Bulk electrolysis and the Electro-separation of zinc(II) were carried out using the setup illustrated in Fig. 1. The pool WE (diameter = 43 mm), CE, and RE (described above) were used. In addition to the electrodes, the system comprised a beaker-type cell (30 mL) and an anion-exchange membrane (Selemion APS, Asahi Glass Engineering Co., Ltd., Japan). The anolyte was circulated in a flow-type optical cell (path length = 2 mm) installed

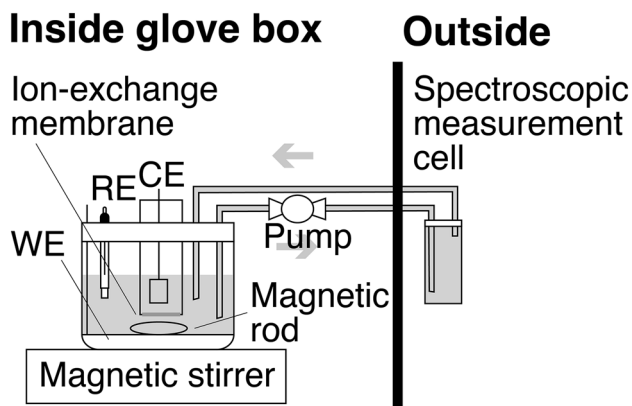


Fig. 1 Schematic setup used for bulk electrolysis

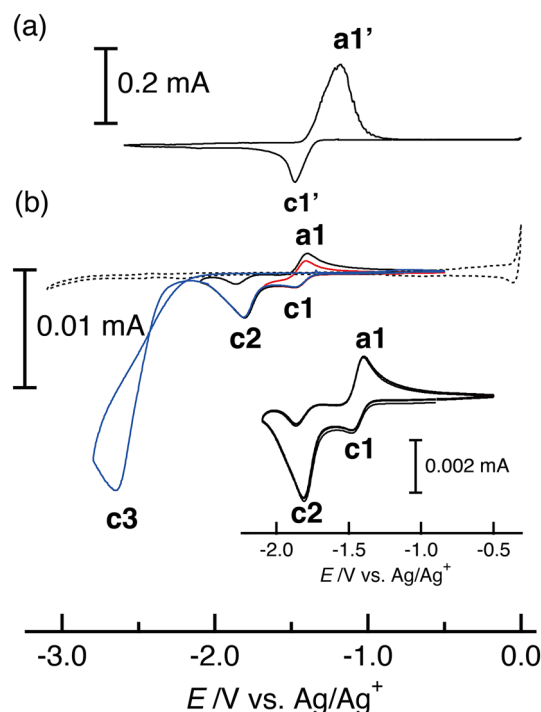


Fig. 2 Cyclic voltammograms of **a** 5 mM $Zn(OTf)_2$ in DMF containing 0.1 M TBAOTf, **b** 5 mM $U(OTf)_4$ in DMF containing 0.1 M TBAOTf (solid line)+the results of three consecutive scans (inset) and DMF containing 0.1 M TBAOTf (dotted line) recorded on the HME at 0.2 V s^{-1} . The sweeps were started at the open-circuit potential and proceeded in the cathodic direction

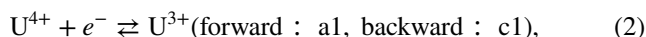
outside the glove box for in situ visible–near-IR spectroscopic measurements (UV-3100PC, Shimadzu). Constant current electrolysis was performed at -5 or -10 mA , and WE potentials were recorded. Each solution ($50 \mu\text{L}$) was sampled at regular intervals and analyzed using ICP-AES to quantify total uranium and zinc(II) concentrations.

3 Results and discussion

3.1 Voltammetric investigation of $U(OTf)_4$ reduction on Hg and Zn(Hg) electrodes

Figure 2 presents the cyclic voltammograms of 5 mM $Zn(OTf)_2$ and 5 mM $U(OTf)_4$ in DMF containing 0.1 M TBAOTf and that of DMF containing 0.1 M TBAOTf (for the potential window survey) recorded on the HME. The potential was scanned at 0.2 V s^{-1} in the cathodic direction starting from the open-circuit potential. The voltammogram of the supporting electrolyte showed that its potential window was sufficient to evaluate the electrode reactions of low-valent uranium triflate and zinc amalgamation. The voltammogram of $Zn(OTf)_2$ showed a single redox wave ($c1'/a1'$; $Zn^{2+} + 2e^- \rightleftharpoons Zn(Hg)$) around $-1.4 \text{ V vs. } Ag/Ag^+$

(hereinafter, all potentials are referenced to Ag/Ag⁺ if not stated otherwise; Fig. 2a). In contrast, the voltammogram of U(OTf)₄ exhibited three cathodic waves (c1, c2, and c3 at –1.48, –1.81, and –2.65 V, respectively) and one anodic wave (a1 at –1.4 V) that disappeared when the potential range was extended beyond –2.1 V in the negative direction (Fig. 2b). The a1 peak current recorded at the reversal potential of –1.7 V (1.25 μA) increased when the potential was set to –2.1 V (1.72 μA). These results suggest that waves c1 and c2 can be attributed to the reduction of two different uranium(IV) species. Moreover, the subsequent reaction of wave c2 was assigned to the degradation of the uranium(III) species generated in wave c2, which increased the content of uranium(III) species oxidized in wave a1. The reduction of U(OTf)₄ in DMF probably involved the following reactions (coordinated DMF molecules are omitted for clarity).



All these reactions except for reaction (4) were sufficiently fast to maintain reproducibility between voltammograms across several scans (Fig. 2, inset). Moreover, the electrode reaction of the uranium(IV) solvate complex (reaction (2)) was quasi-reversible (Figs. S2 and S3, Table S1), and this complex accounted for only 24% of all uranium(IV) species in solution (Fig. S4). However, this reaction may have substantially overlapped with zinc amalgamation/dissolution.

To compare the electrode reactions of pure and zinc-amalgamated Hg, CV measurements were also conducted on Zn(Hg) for 5 mM U(OTf)₄ in DMF containing 0.1 M TBAOTf and for DMF containing 0.1 M TBAOTf (Fig. 3). The potential scans were carried out as in the case of the HME, namely in the cathodic direction from the open-circuit potential at a sweep rate of 0.2 V s⁻¹, and showed that the positive side of the potential window was restricted by the onset of zinc(II) dissolution from Zn(Hg) at –1.55 V. The voltammogram of the U(OTf)₄ solution exhibited three cathodic waves (c1', c2, and c3 at –1.52, –1.80, and –2.60 V, respectively) with peak potentials consistent with those observed for the HME (Fig. 2). However, the c1' peak current of the second and third cycles exceeded that of the first cycle (Fig. 3, inset), in contrast to wave c1 on HME (Fig. 2 inset). Moreover, a similar peak was observed during the potential window measurement. Based on these results, wave c1' was assigned to zinc amalgamation. It is important

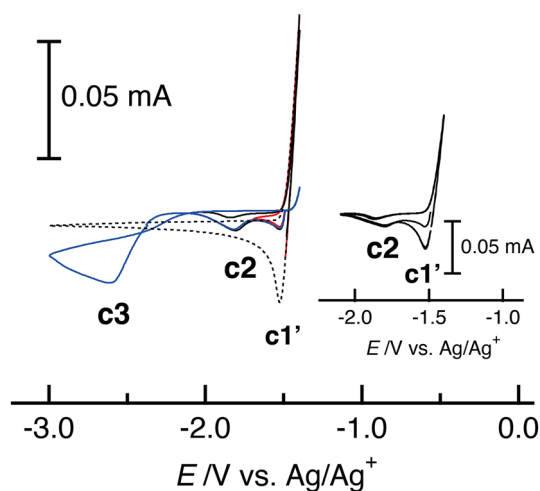


Fig. 3 Cyclic voltammograms of 5 mM U(OTf)₄ in DMF containing 0.1 M TBAOTf+the results of three consecutive scans (inset) and of DMF containing 0.1 M TBAOTf (dotted line) recorded at 0.2 V s⁻¹ on Zn(Hg). The sweeps were started at the open-circuit potential and proceeded in the cathodic direction

to note that the competing reduction of the uranium(IV) solvate complex (wave c1) was expected to occur at the same potential.

3.2 Bulk electrolysis of U(OTf)₄ in DMF on Hg and Zn(Hg) electrodes

To investigate the electrode reduction of low-valent uranium triflate and zinc(II) on the large-area WE, we performed the bulk electrolysis of U(OTf)₄ on Hg and Zn(Hg) in DMF and compared the results with those of Voltammetric experiments.

Figure 4 shows the solution-phase behavior of uranium(III) and zinc(II) (i.e., the evolution of [U³⁺]/[U]_{total} and [Zn²⁺]) and that of WE potential during the bulk electrolysis of 6.4 mM U(OTf)₄ (hereinafter abbreviated as “without Zn(OTf)₂”) and a mixture of 6.7 mM U(OTf)₄ + 4.6 mM Zn(OTf)₂ (“with Zn(OTf)₂”) in DMF containing 0.1 M TBAOTf at –10 mA. [U³⁺] was calculated from the intensity of uranium(III) absorption at 11,062 cm⁻¹ measured during electrolysis (Fig. S5) and the corresponding molar extinction coefficient (estimated as 436 M⁻¹ cm⁻¹; Fig. S1).

In the case of “without Zn(OTf)₂,” the [U³⁺]/[U]_{total} ratio saturated at <0.2 about 20 min after the onset of electrolysis. Similar results were obtained using other uranium(III) absorption bands (at 8130, 9242, 9469, 10,121, 13,440, 16,025, and 18,587 cm⁻¹), whereas the uranium(IV) bands (at 7000, 9500, and 12,500 cm⁻¹) monotonically lost intensity (Fig. S5). The WE potential curve showed one precipitous shoulder (–1.8 V) and one plateau (–2.3 V). There

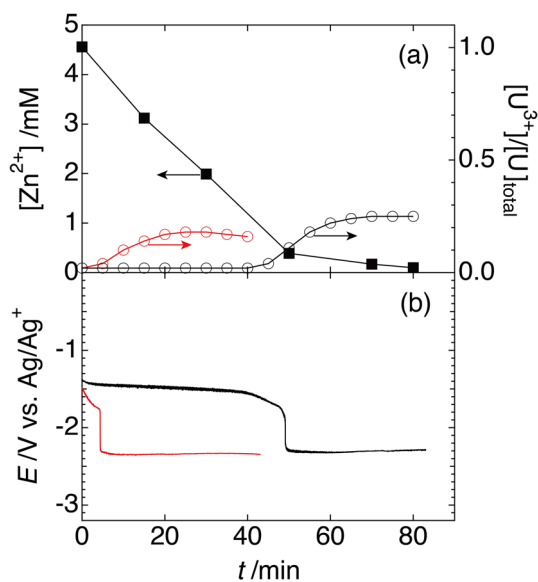


Fig. 4 Changes in (a) $[Zn^{2+}]$ and $[U^{3+}]/[U]_{total}$ and (b) the electrode potential of Hg during constant current (-10 mA) electrolytic reduction of 6.4 mM $U(OTf)_4$ (red) or a mixture of 6.7 mM $U(OTf)_4$ + 4.6 mM $Zn(OTf)_2$ (black) in DMF containing 0.1 M TBAOTf. (Color figure online)

was no signal around -1.4 V related to uranium(IV) solvate reduction (reaction (2)). The shoulder, assigned to the reduction of $[U(OTf)]^{3+}$ (reaction (3)), was too narrow for this reduction to be complete, as assumed from previous Voltammetric investigations. Moreover, the plateau potential of -2.3 V, corresponding to the continuous reduction of uranium(IV) and the preservation of uranium(III) species on the plateau following their first generation, has never been observed in CV and NPV experiments. These results indicate that the reduction behavior of $U(OTf)_4$ on the large-area WE (diameter = 43 mm) used in bulk electrolysis is significantly different from that on the small-area WE (area ≈ 1.4 mm²) used in Voltammetric experiments.

In the case of “with $Zn(OTf)_2$,” $[Zn^{2+}]$ rapidly decreased over the first 50 min, subsequently more slowly decreasing to 0.1 mM. The $[U^{3+}]/[U]_{total}$ ratio started to increase after 40 min and saturated at 0.25 after 70 min. On the other hand, the WE potential curve showed one shoulder (-1.8 V) and two plateaus (-1.5 and -2.3 V), respectively. The first plateau potential well matched that of zinc amalgamation observed in CV experiments and the period agreed with the abovementioned decrease of $[Zn^{2+}]$. Moreover, the reactions of the other plateau and shoulder were essentially identical to those observed “without $Zn(OTf)_2$,” whereas the time of $[U(OTf)]^{3+}$ reduction was obviously longer in the latter case.

Figure 5 presents the changes in $[U^{3+}]/[U]_{total}$, $[Zn^{2+}]$, and WE potential during the bulk electrolysis of 5.2 mM $U(OTf)_4$ in DMF containing 0.1 M TBAOTf with $Zn(Hg)$ as

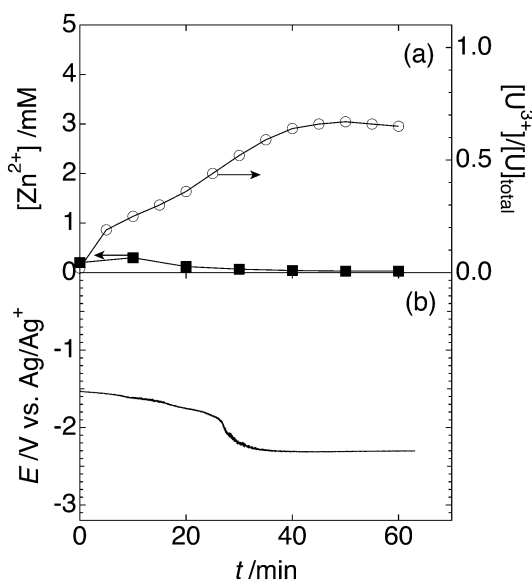


Fig. 5 Changes in (a) $[Zn^{2+}]$ and $[U^{3+}]/[U]_{total}$ and (b) the electrode potential of $Zn(Hg)$ during constant current (-5 mA) electrolytic reduction of 5.2 mM $U(OTf)_4$ in DMF containing 0.1 M TBAOTf

the WE at -5 mA. The behavior of $[Zn^{2+}]$ indicated that the slight occurrence of zinc amalgamation was followed by zinc dissolution from $Zn(Hg)$ in the first 20 – 25 min. Simultaneously, uranium(III) was generated up to $[U^{3+}]/[U]_{total} = 0.44$ by the reduction of uranium(IV) (Fig. S6) and the $[U^{3+}]/[U]_{total}$ ratio saturated at 0.66 after 45 min. The WE potential curve exhibited a gradual slope from -1.5 to -1.8 V and one plateau at -2.3 V. These results indicated that the potential slope observed for the first 25 min corresponded to the competing reactions of zinc amalgamation and the electrolytic reduction of uranium(IV) to uranium(III). However, when zinc amalgamation was almost complete, the electrolytic generation of uranium(III) became difficult and finally stopped, whereas the reduction of uranium(IV) monotonically continued (Fig. S6) in the plateau region at -2.3 V.

The results of bulk electrolysis experiments demonstrated that the WE potential of zinc amalgamation was consistent with the results of Voltammetric experiments, in contrast to that of the electrochemical reactions of low-valent uranium triflate. Notably, the former potential was more positive than the latter, especially for the plateau potential at -2.3 V, which was related to uranium(III) degradation.

3.3 Electroseparation of zinc(II) from uranium(III) solution on $Zn(Hg)$

After the reduction of 4.5 mM $U(OTf)_4$ in DMF by $Zn(Hg)$, we attempted the Electroseparation of zinc(II) from the uranium(III) solution by bulk electrolysis on $Zn(Hg)$.

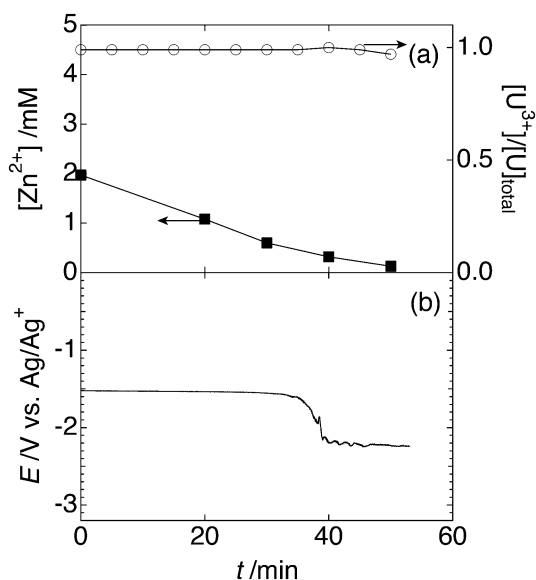


Fig. 6 Changes in (a) $[Zn^{2+}]$ and $[U^{3+}]/[U]_{total}$ and (b) the electrode potential of Zn(Hg) during the Electroseparation of zinc(II) from DMF containing 4.5 mM uranium triflate after reduction by Zn(Hg)

Figure 6 shows the concentrations of uranium(III) and zinc(II) ($[U^{3+}]/[U]_{total}$ and $[Zn^{2+}]$) and the WE potential as functions of time, revealing that $[Zn^{2+}]$ monotonically decreased and reached 0.13 mM at 50 min. In contrast, the $[U^{3+}]/[U]_{total}$ ratio was stable at 0.99 for 35 min and was comparable to that obtained just after reduction by Zn(Hg) ($[U^{3+}]/[U]_{total} = 1.00$ at 40 min), subsequently experiencing a slight decrease. Similar results were obtained from other uranium(III) absorption bands (Fig. S7). The WE potential curve showed that zinc amalgamation occurring at the first plateau of -1.52 V, as assigned by CV experiments, exclusively proceeded up to 35 min. At times of 35–40 min, the potential shifted in the negative direction from the first plateau to the second plateau located at approximately -2.3 V. In this range, spectroscopic observations indicated the occurrence of competitive zinc amalgamation and uranium(IV) (presumably $U(OTf)^{3+}$) reduction. The second plateau ($t > 40$ min) reflected the degradation of uranium(III) without uranium amalgamation corresponding to the potential of -2.6 V (reaction (4)).

The coulombic efficiency (η_C) of zinc(II) Electroseparation (i.e., zinc amalgamation) is estimated as:

$$\eta_C = \frac{(C_{i-1} - C_i)V}{(q_i - q_{i-1})/nF}, \quad (5)$$

where C_i and C_{i-1} are the concentrations of $[Zn^{2+}]$ in samples i and $i-1$ ($i = 1, 2, \dots$), V is the solution volume (L), q_i and q_{i-1} are the integral quantities of electricity consumed

Table 1 Coulombic efficiency (η_C) and zinc(II) separation ratios achieved at different times

Sample number (i)	Sampling time (min)	η_C	Separation ratio (%)
1	20	0.86	45.2
2	30	0.93	69.5
3	40	0.54	83.8
4	50	0.37	93.4

during electrolysis (C), F is the Faraday constant, and n is the stoichiometric number of electrons involved in the electrode reaction ($n = 2$ for the reduction of zinc(II)). Simultaneously, the zinc(II) separation ratio is estimated as:

$$\text{Separation ratio} = (1 - C_i/C_0) \times 100\%, \quad (6)$$

where C_0 is $[Zn^{2+}]$ at the beginning of electrolysis. Table 1 lists the thus obtained values, revealing that the highest η_C equaled 0.93, while the final zinc(II) separation ratio equaled 93.4%. These results demonstrate that almost quantitative zinc(II) removal from the uranium(III) solution occurred under the chosen conditions.

4 Conclusion

The reduction of $U(OTf)_4$ in DMF containing TBAOTf was studied on the pristine HME and on the HME where Hg was replaced with Zn(Hg). The three cathodic waves observed in the former case were assigned to the reduction of a uranium(IV) solvate complex and $[U(OTf)]^{3+}$ (-1.48 and -1.81 V, respectively) and uranium amalgamation (-2.65 V). The redox wave of the uranium(IV) solvate complex overlapped with those of zinc(II) dissolution from Zn(Hg) and zinc amalgamation. The electrode reactions of low-valent uranium triflate on the large-area WE (used for bulk electrolysis) were critically different from those observed on the small-area WE (used for Voltammetric experiments), in contrast to the electrode reaction of zinc(II). Notably, a new plateau potential related to uranium(III) degradation was obtained around -2.3 V instead of a lack of uranium(IV) solvate complex reduction under all conditions. These results demonstrated that zinc amalgamation proceeded prior to uranium(III) degradation. The Electroseparation of zinc(II) from the uranium(III) solution prepared by the reduction of $U(OTf)_4$ using Zn(Hg) in DMF was conducted in a quantitative manner, with the final zinc(II) separation ratio equaling 93.4%. The results show that Electroseparation has sufficient potential for the preparation of spent reductant-free uranium(III) starting materials. We are currently attempting to demonstrate this method using THF,

which is typical synthetic solvent, and subsequent synthesis of uranium(III) complexes.

Supplementary Information The online version contains supplementary material available at <https://doi.org/10.1007/s10800-022-01698-7>.

Acknowledgements The author would like to express great acknowledgements to Prof. Tomoo Yamamura (Inst. for Integrated Radiation and Nuclear Science, Kyoto Univ.) and late associate Prof. Isamu Satoh for their kind encouragements and supports. This work was partly supported by JSPS KAKENHI [Grant No. 19760607].

Declarations

Conflict of interest There are no conflicts of interest to declare.

References

- Ephritikhine M (2006) The vitality of uranium molecular chemistry at the dawn of the XXIst century. *Dalton Trans* 21:2501–2516. <https://doi.org/10.1039/b603463b>
- Korobkov I, Gorelsky S, Gambarotta S (2009) Reduced uranium complexes: synthetic and DFT study of the role of pi ligation in the stabilization of uranium species in a formal low-valent state. *J Am Chem Soc* 131(30):10406–10420. <https://doi.org/10.1021/ja9002525>
- Antunes MA, Pereira LC, Santos IC, Mazzanti M, Marcalo J, Almeida M (2011) $[U(Tp(Me_2)_2(bipy))]^+$: a cationic uranium(III) complex with single-molecule-magnet behavior. *Inorg Chem* 50(20):9915–9917. <https://doi.org/10.1021/ic200705p>
- Mansell SM, Kaltsoyannis N, Arnold PL (2011) Small molecule activation by uranium tris(aryloxides): experimental and computational studies of binding of N_2 , coupling of CO, and deoxygenation insertion of CO_2 under ambient conditions. *J Am Chem Soc* 133(23):9036–9051. <https://doi.org/10.1021/ja2019492>
- Hohloch S, Garner ME, Parker BF, Arnold J (2017) New supporting ligands in actinide chemistry: tetramethyltetraazaannulene complexes with thorium and uranium. *Dalton Trans* 46(40):13768–13782. <https://doi.org/10.1039/c7dt02682j>
- Boreen MA, Arnold J (2020) The synthesis and versatile reducing power of low-valent uranium complexes. *Dalton Trans* 49(43):15124–15138. <https://doi.org/10.1039/d0dt03151h>
- Boreen MA, Gould CA, Booth CH, Hohloch S, Arnold J (2020) Structure and magnetism of a tetrahedral uranium(III) beta-diketiminate complex. *Dalton Trans* 49(23):7938–7944. <https://doi.org/10.1039/d0dt01599g>
- Riedhammer J, Aguilar-Calderon JR, Miehlich M, Halter DP, Munz D, Heinemann FW, Fortier S, Meyer K, Mindiola DJ (2020) Werner-type complexes of uranium(III) and (IV). *Inorg Chem* 59(4):2443–2449. <https://doi.org/10.1021/acs.inorgchem.9b03229>
- Clark DL, Sattelberger AP, Bott SG, Vrtis RN (1989) Lewis base adducts of uranium triiodide: a new class of synthetically useful precursors for trivalent uranium chemistry. *Inorg Chem* 28(10):1771–1773. <https://doi.org/10.1021/ic00309a004>
- Drożdżyński J (2005) Tervalent uranium compounds. *Coord Chem Rev* 249(21):2351–2373. <https://doi.org/10.1016/j.ccr.2005.05.016>
- Carmichael CD, Jones NA, Arnold PL (2008) Low-valent uranium iodides: straightforward solution syntheses of UI_3 and UI_4 etherates. *Inorg Chem* 47(19):8577–8579. <https://doi.org/10.1021/ic801138e>
- Fetrow TV, Grabow JP, Leddy J, Daly SR (2021) Convenient syntheses of trivalent uranium halide starting materials without uranium metal. *Inorg Chem* 60(11):7593–7601. <https://doi.org/10.1021/acs.inorgchem.1c00598>
- Avens LR, Bott SG, Clark DL, Sattelberger AP, Watkin JG, Zwick BD (1994) A convenient entry into trivalent actinide chemistry: synthesis and characterization of $AnI_3(THF)_4$ and $An[N(SiMe_3)_2]_3$ ($An = U, Np, Pu$). *Inorg Chem* 33(10):2248–2256. <https://doi.org/10.1021/ic00088a030>
- Evans WJ, Kozimor SA, Ziller JW, Fagin AA, Bochkarev MN (2005) Facile syntheses of unsolvated UI_3 and tetramethylcyclopentadienyl uranium halides. *Inorg Chem* 44(11):3993–4000. <https://doi.org/10.1021/ic0482685>
- Monreal MJ, Thomson RK, Cantat T, Travia NE, Scott BL, Kiplinger JL (2011) $UI_4(1,4\text{-dioxane})_2$, $[UCl_4(1,4\text{-dioxane})]_2$, and $UI_3(1,4\text{-dioxane})_{1.5}$: stable and versatile starting materials for low- and high-valent uranium chemistry. *Organometallics* 30(7):2031–2038. <https://doi.org/10.1021/om200093q>
- Schleid T, Meyer G, Morss LR (1987) Facile synthesis of UCl_4 and $ThCl_4$, metallothermic reductions of UCl_4 with alkali metals and crystal structure refinements of UCl_3 , UCl_4 and Cs_2UCl_6 . *J Less Common Met* 132(1):69–77. [https://doi.org/10.1016/0022-5088\(87\)90175-5](https://doi.org/10.1016/0022-5088(87)90175-5)
- La Pierre HS, Heinemann FW, Meyer K (2014) Well-defined molecular uranium(III) chloride complexes. *Chem Commun (Camb)* 50(30):3962–3964. <https://doi.org/10.1039/c3cc49452g>
- Bullock JI, Storey AE (1977) Complexes of uranium(III) with bidentate amides. *J Chem Soc Chem Commun*. <https://doi.org/10.1039/c39770000507>
- Moody DC, Odom JD (1979) The chemistry of trivalent uranium: the synthesis and reaction chemistry of the tetrahydrofuran adduct of uranium trichloride, $UCl_3(THF)_x$. *J Inorg Nucl Chem* 41(4):533–535. [https://doi.org/10.1016/0022-1902\(79\)80439-X](https://doi.org/10.1016/0022-1902(79)80439-X)
- Moody DC, Zozulin AJ, Salazar KV (1982) Improved synthesis of $UCl_3(THF)_x$ and the preparation of 15-crown-5 derivatives of trivalent uranium. *Inorg Chem* 21(10):3856–3857. <https://doi.org/10.1021/ic00140a055>
- Rossetto G, Zanella P, Paolucci G, De Paoli G (1982) The reduction of uranium tetrachloride by lithium tetrahydroaluminate in tetrahydrofuran or dimethoxyethane. *Inorg Chim Acta* 61:39–42. [https://doi.org/10.1016/S0020-1693\(00\)89116-1](https://doi.org/10.1016/S0020-1693(00)89116-1)
- Berthet J-C, Lance M, Nierlich M, Vigner J, Ephritikhine M (1991) Tricyclopentadienyluranium azide complexes. *J Organomet Chem* 420(2):C9–C11. [https://doi.org/10.1016/0022-328x\(91\)80271-k](https://doi.org/10.1016/0022-328x(91)80271-k)
- Hauchard D, Cassir M, Chivot J, Ephritikhine M (1991) Electrochemical study of uranium(IV) and uranium(III) organometallic compounds in tetrahydrofuran by means of conventional microelectrodes and ultramicroelectrodes. *J Electroanal Chem Interfacial Electrochem* 313(1–2):227–241. [https://doi.org/10.1016/0022-0728\(91\)85182-o](https://doi.org/10.1016/0022-0728(91)85182-o)
- Mech A, Karbowski M, Lis T, Drożdżyński J (2006) Monomeric, dimeric and polymeric structure of the uranium trichloride hydrates. *Polyhedron* 25(10):2083–2092. <https://doi.org/10.1016/j.poly.2006.01.004>
- Daly SR, Girolami GS (2010) Synthesis, characterization, and structures of uranium(III) N,N -dimethylaminodiboranates. *Inorg Chem* 49(11):5157–5166. <https://doi.org/10.1021/ic100290j>
- Hart FA, Tajik M (1983) Complexes of uranium(III) with cyclic polyethers and with aromatic diamines. *Inorg Chim Acta* 71:169–173. [https://doi.org/10.1016/s0020-1693\(00\)83655-5](https://doi.org/10.1016/s0020-1693(00)83655-5)
- Kennedy JH (1960) Determination of uranium(IV) by reduction to uranium(III) in Jones reductor. *Anal Chem* 32(2):150–152. <https://doi.org/10.1021/ac60158a002>

28. Satō A (1967) Studies of the behavior of trivalent uranium in an aqueous solution. I. Its reduction and its stability in various acid solutions. *Bull Chem Soc Jpn* 40(9):2107–2110. <https://doi.org/10.1246/bcsj.40.2107>
29. Drożdżyński J (1978) Absorption spectra of uranium(+ 3) in solution. *J Inorg Nucl Chem* 40(2):319–323. [https://doi.org/10.1016/0022-1902\(78\)80131-6](https://doi.org/10.1016/0022-1902(78)80131-6)
30. Drożdżyński J (1984) Spectroscopic investigations of some uranium(III) complexes. *J Mol Struct* 114:449–454. [https://doi.org/10.1016/0022-2860\(84\)87184-7](https://doi.org/10.1016/0022-2860(84)87184-7)
31. Yamamura T, Shirasaki K, Shiokawa Y (2006) Preparation of uranium(III) triflate in tetrahydrofuran by reduction of $U(OTf)_4$ with zinc amalgam. *J Phys Soc Jpn* 75(Suppl):149–151. <https://doi.org/10.1143/jpsjs.75s.149>
32. Shen M, Li B, Li SZ, Yu JG (2011) Electrochemical removal of $AlCl_3$ from LiCl-KCl Melts. *Metall Mater Trans A* 43(5):1662–1669. <https://doi.org/10.1007/s11661-011-0982-7>
33. Shen M, Li B, Yu J (2012) Investigation on electrochemical removal of $CaCl_2$ from LiCl-KCl melts. *Electrochim Acta* 62:153–157. <https://doi.org/10.1016/j.electacta.2011.12.007>
34. Liu K, Liu Y-L, Chai Z-F, Shi W-Q (2021) Electrochemical separation of uranium from lanthanides (La, Ce, Pr, Nd and Sm) on liquid gallium electrode. *Sep Purif Technol* 265:118524. <https://doi.org/10.1016/j.seppur.2021.118524>
35. Chen GZ, Fray DJ (2001) Cathodic refining in molten salts: removal of oxygen, sulfur and selenium from static and flowing molten copper. *J Appl Electrochem* 31(2):155–164. <https://doi.org/10.1023/A:1004175605236>
36. Zhao X, Liu H, Li A, Shen Y, Qu J (2012) Bromate removal by electrochemical reduction at boron-doped diamond electrode. *Electrochim Acta* 62:181–184. <https://doi.org/10.1016/j.electacta.2011.12.013>
37. Giridhar P, Venkatesan KA, Subramaniam S, Srinivasan TG, Vasudeva Rao PR (2008) Extraction of uranium (VI) by 1.1 M tri-n-butylphosphate/ionic liquid and the feasibility of recovery by direct electrodeposition from organic phase. *J Alloy Compd* 448(1–2):104–108. <https://doi.org/10.1016/j.jallcom.2007.03.115>
38. Jagadeeswara Rao C, Venkatesan KA, Nagarajan K, Srinivasan TG, Vasudeva Rao PR (2011) Electrodeposition of metallic uranium at near ambient conditions from room temperature ionic liquid. *J Nucl Mater* 408(1):25–29. <https://doi.org/10.1016/j.jnucmat.2010.10.022>
39. Ohashi Y, Harada M, Asanuma N, Ikeda Y (2015) Feasibility studies on electrochemical recovery of uranium from solid wastes contaminated with uranium using 1-butyl-3-methylimidazolium chloride as an electrolyte. *J Nucl Mater* 464:119–127. <https://doi.org/10.1016/j.jnucmat.2015.04.024>
40. Krishna GM, Suneesh AS, Venkatesan KA, Antony MP (2016) Electrochemical interference of some fission products during the electrodeposition of uranium oxide from 1-butyl-3-methylimidazolium chloride ionic liquid. *J Electroanal Chem* 780:225–232. <https://doi.org/10.1016/j.jelechem.2016.09.035>
41. Sakamura Y, Omori T, Inoue T (2017) Application of electrochemical reduction to produce metal fuel material from actinide oxides. *Nucl Technol* 162(2):169–178. <https://doi.org/10.13182/nt162-169>
42. Herrmann SD, Li SX (2017) Separation and recovery of uranium metal from spent light water reactor fuel via electrolytic reduction and electrorefining. *Nucl Technol* 171(3):247–265. <https://doi.org/10.13182/nt171-247>
43. Behr B, Taraszewska J, Stroka J (1975) Kinetics of Zn^{2+} reduction at a Hg electrode from water-acetone and water-methanol mixtures. *J Electroanal Chem Interfacial Electrochem* 58(1):71–80. [https://doi.org/10.1016/s0022-0728\(75\)80346-9](https://doi.org/10.1016/s0022-0728(75)80346-9)
44. Andreu R, Sluyters-Rehbach M, Remijnse AG, Sluyters JH (1982) The mechanism of the reduction of $Zn(II)$ from $NaClO_4$ base electrolyte solutions at the DME. *J Electroanal Chem Interfacial Electrochem* 134(1):101–115. [https://doi.org/10.1016/s0022-0728\(82\)85030-4](https://doi.org/10.1016/s0022-0728(82)85030-4)
45. Taraszewska J, Wałęga A (1986) Medium effect: kinetics of Zn^{2+} reduction at the Hg electrode from water + dimethylformamide mixtures. *J Electroanal Chem Interfacial Electrochem* 200(1–2):261–277. [https://doi.org/10.1016/0022-0728\(86\)90060-4](https://doi.org/10.1016/0022-0728(86)90060-4)
46. Michlmayr M, Gritzner G, Gutmann V (1966) Polarographic studies on uranium compounds in dimethylformamide and dimethylsulfoxide. *Inorg Nuclear Chem Lett* 2(8):227–231. [https://doi.org/10.1016/0020-1650\(66\)80033-8](https://doi.org/10.1016/0020-1650(66)80033-8)
47. Shirasaki K, Yamamura T, Herai T, Shiokawa Y (2006) Electrodeposition of uranium in dimethyl sulfoxide and its inhibition by acetylacetone as studied by EQCM. *J Alloy Compd* 418(1–2):217–221. <https://doi.org/10.1016/j.jallcom.2005.10.059>
48. Shirasaki K, Yamamura T, Monden Y, Shiokawa Y (2006) Electrolytic reduction of $U(IV)$ salts to $U(III)$ in *N,N*-dimethylformamide: effects of electrode materials and counter anions. *J Phys Soc Jpn* 75(Suppl):152–154. <https://doi.org/10.1143/jpsjs.75s.152>
49. Izutsu K (2002) Redox Reactions in Non-Aqueous Solvents. Wiley-VCH Verlag GmbH & Co. KGaA, Weinheim

Publisher's note Springer Nature remains neutral with regard to jurisdictional claims in published maps and institutional affiliations.